Physical modeling of the dam-break flow of sedimenting suspensions

L. Girolami, Frédéric Risso

Physical modeling of the dam-break flow of sedimenting suspensions

Laurence Girolami*

Laboratoire GéHCO, Campus Grandmont,

Université de Tours, 37200 Tours, France

Frédéric Risso†

Institut de Mécanique des Fluides de Toulouse (IMFT),

Université de Toulouse, CNRS, 31400 Toulouse, France

(Dated: January 21, 2020)

Abstract

We develop a physical model of the dam-break flow of fine non-cohesive particles initially fluidized by a gas. By revisiting previous experiments, we show that the dynamics of such flows involves two uncoupled phenomena. On the one hand, the settling of the particles is the same as that of a non-flowing suspension, so that the mass flux of particles that deposit can be related to the sole properties of the suspension. On the other hand, the flow of the gas-particle mixture is similar to that of an equivalent fluid of constant density and low viscosity. The momentum lost by the flowing mixture is thus the product of the deposited mass flux by the longitudinal velocity. These properties allow us to model the time duration of the flow as the time taken by the particles to settle and the slope of the final deposit as the ratio between the growth rate of the deposit height and the velocity of the front of the dam-break flow. Finally, these findings lead to the formulation of consistent shallow-water equations involving specific terms of mass and momentum transfer at the bottom wall, which can be used to compute the dense lower layer of ash flows generated by a volcanic eruption. They also provide tools for the interpretation of field measurements by geologists.

I. INTRODUCTION

The fluidization of fine non-cohesive powders by a gas can lead to the formation of a dense, homogeneously expanded suspension that deflates and settles progressively once the gas supply is vanished. The mobility of such fluidized mixtures can be considerable, especially when they travel large distances down gentle slopes, as usually observed in some catastrophic episodes of explosive volcanic eruptions. They represent thereby one of the most important natural hazards encountered in geophysics [1–3]. The physical description of these flows has become a major issue for the prediction of both the eruption time and the surface affected by the deposits, which may depend on the initial conditions at the vent. This step requires therefore the determination of relevant scaling laws that may be achieved first through an experimental analysis, performed in a well-controlled geometry, such as a rectangular dam-break channel which reasonably enables to both generate a dense

* laurence.girolami@univ-tours.fr

† frisso@imft.fr

homogeneous suspension in the locked reservoir as well as a gravitational sedimenting current that travels down the channel [4–12].

Previous studies, conducted in this way, have revealed important features of these flows. Once released down the channel, the suspension collapses from a height h_0 to form a quasi-inviscid current, the front of which travels at a quasi-constant speed $U_{\mathcal{F}}$ that scales with the gravitational velocity $\sqrt{gh_0}$ [8–12]. As the mixture is flowing, the particles sediment at a velocity U_{sed} and form a deposit at the bottom of the channel that grows at a velocity U_{agg}. Surprisingly, the values of U_{sed} and U_{agg} measured during the mixture is flowing are found to be constant both in time and all along the channel [12–15]. Moreover, they are also equal to those determined in the same mixture sedimenting while confined without flowing within the locked reservoir. This remarkable result allows the authors to claim that ash particles within dense natural pyroclastic flows settle at a rate that could be predicted independently of the flow dynamics. Altogether, these results suggest that the flow of the mixture through the channel, hereafter referred to as *dam-break flow*, and the settling of the particles, hereafter referred to as *particle sedimentation*, are very weakly coupled.

The objective of the present study is to propose a physical analysis of these results in order to build a predictive model. By assuming that dam-break and particle sedimentation are independent, we derive mathematical expressions that relate together the global characteristics of the phenomenon: front velocity $U_{\mathcal{F}}$, sedimenting velocity U_{sed}, overall flow duration T, height h_{d_∞} and length L of the final deposit. These relations are validated by revisiting previous laboratory experiments conducted with volcanic ash by one of the authors [12–15]. They can be used by volcanologists to infer the flow characteristics from the properties of a deposit. In addition, they can also provide a model for the mass and momentum transfers between the flowing mixture and the bottom wall, which enables the way to shallow-water numerical simulations of pyroclastic flows that travel down variable slopes.

The paper is organized as follows. Section II presents the flow configuration and known results. Section III develops the physical model and compare its predictions to experimental results. Consequences upon the modelling of the flow mixture are drawn in section IV. Final discussion and conclusions are set out in section V.

II. REFERENCE FLOW CONFIGURATION AND KNOWN RESULTS

Despite the multiplication of sophisticated models able to reasonably compute the behaviour of turbulent dilute surges [16–21], simulations developed for dense pyroclastic flows still lack of a realistic description, in particular through the term of bottom friction employed to capture the deceleration and stop of the flows during their final course [22–25]. Such a scientific lock needs to be addressed first experimentally in order to capture the main features of these flows and to relate the initial suspension geometry and properties to those of the final deposit. Dam-break flow configurations, commonly used in this purpose [9, 12], turn out to be the more consistent tool able to provide a local description of the flow and particles trajectories, and thus to infer the key parameters that govern such sedimenting suspensions. Specifically, they can help to understand how the mixture properties can control the pyroclastic flow dynamics.

Figure 1 describes the successive steps of a typical experiment of the dam-break flow of a fluidized suspension. First, the particles are poured into a locked reservoir in order to form a packed bed of height h_{d_0} and solid fraction Φ_{pack} (fig 1a). Then, a gas is supplied from the bottom at a given velocity such as the suspension expands to height h_0 at volume fraction Φ_s (fig 1a). Note that homogenous gas-particles suspensions over a large range of expansion (typically $0.65 \leq h_{d_0}/h_0 = \Phi_s/\Phi_{pack} \leq 0.95$) can only be achieved with non-cohesive material belonging to group A in Geldart classification [26], such as volcanic ash particles which need to be heated to 180°C to join this group [12]. From that point, two kinds of experiments can be carried out: a first non-flowing defluidization process is performed by stopping the gas injection while the reservoir remains locked (fig 1c); a second flowing and defluidization process is obtained by opening the channel gate simultaneously to the stop of fluidization (fig 1d).

The sedimentation velocity in the non-flowing case (fig 1c) has been recently analyzed [27] for fine heated particles including volcanic ash of random shape and almost spherical synthetic particles (FCC). In any case, it is well described by the following semi-empirical expression,

$$U_{sed} = \frac{U_{ref}}{8.6}\left(1 - \frac{\Phi_s}{\Phi_{pack}}\right)^{0.45} \quad \text{with} \qquad U_{ref} = \frac{g\rho_s\,(1-\Phi_s)\,d^2}{18\;\mu_f}\,, \tag{1}$$

where g is the gravity acceleration, ρ_s the density of solid particle material, μ_f the gas viscosity and d the average diameter of the particles. In particular, this result shows that

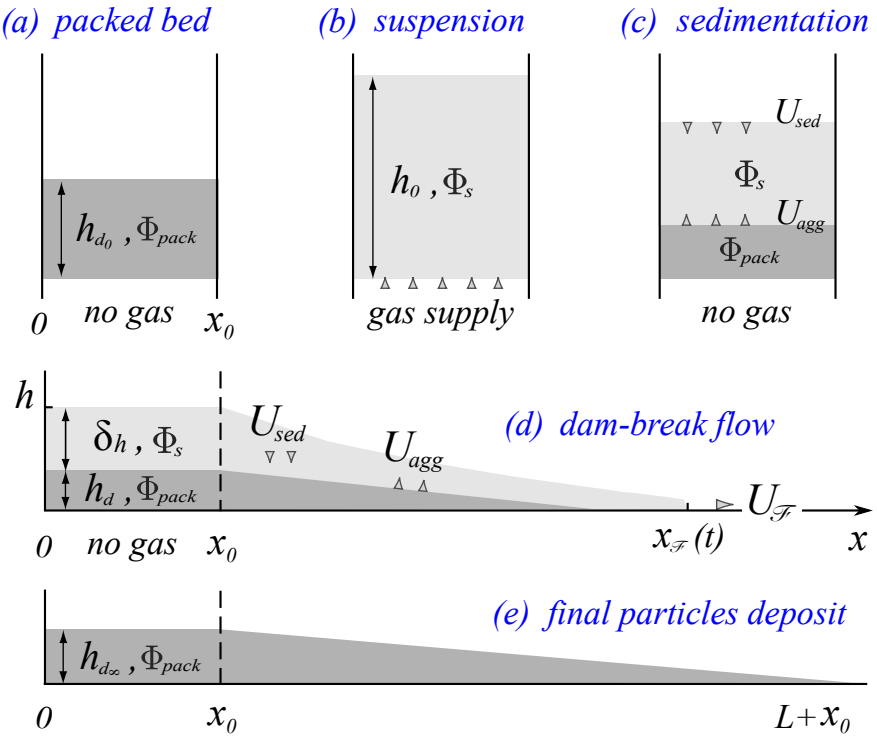

FIG. 1. Schemes of the various experimental configurations: (a) packed state; (b) homogeneously fluidized and expanded suspension; (c) non-flowing defluidization process; (d) simultaneous flow and defluidization process performed through the dam-break flow; (e) final packed deposit after flow has ceased.

the particle volume fraction at packing, Φ_{pack}, is sufficient to encapsulate all the geometric properties of the volcanic ash.

When the gate is opened, the particle sedimentation is initiated simultaneously to the dam-break flow (figs 1d and 2). The fluidization technique, which enables to significantly vary Φ_s within the mixture [27], allows to distinguish the dynamics of dry granular materials governed by frictional interactions [9, 28] from that of significantly expanded suspensions [8, 12]. Let us focus on the second case, which is the subject of the present study. Regarding the sedimentation, U_{sed} is found to be the same as in the non-flowing case [12–15] and can therefore still be described by eq 1. Regarding the dam-break flow, it involves three phases that can be distinguished by considering the velocity $U_{\mathcal{F}}$ of the front [8, 12]: a brief initial acceleration associated with the column collapse, a second phase where the front velocity remains constant ($U_{\mathcal{F}} = U_{\mathcal{F}_2}$), and a final deceleration that lasts until the flow ceases. These

features are similar to those of a dam-break flow of water [29] with a second phase that is largely dominant and involves a velocity that is determined by gravity: $U_{\mathcal{F}_2} = k\sqrt{gh_0}$. The specific value of k, which depends in a complex way on the initial column collapse, has not been modelled so far. It is observed to vary approximately between the value $k = \sqrt{2}$ corresponding to a vertical free fall and the value $k = 2$ associated with a dam-break under shallow-water condition [7, 30].

At the end of the process, the particles form a deposit characterized by a maximal height h_{d_∞} and a total length $L + x_0$ (fig 1e).

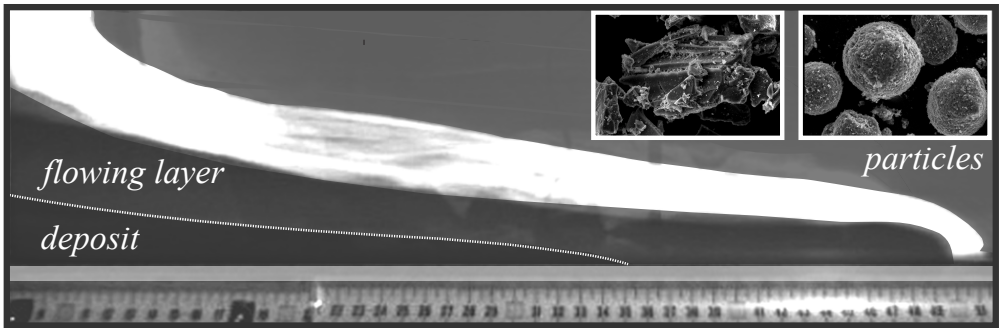

FIG. 2. Picture of the dam-break flow of an expanded suspension of volcanic ash heated at 180°C. The two inserts are pictures of volcanic ash (on the left) and FCC particles (on the right).

In the next section, we shall formulate physical hypotheses based on the known features previously reminded and that will allow us to derive expressions able to relate the initial conditions of the mixture (h_{d_0},Φ_s,Φ_{pack},U_{ref}) to the global properties of the flow (U_{sed},T) and of the final deposit (h_{d_∞},L). The validity of this model will be assessed by revisiting the experiments conducted by Girolami [13], which consisted in releasing highly expanded suspensions made with hot volcanic ash and gas from a reservoir down to an impermeable channel (figs 1d,e). These experiments were presented in detail in a series of articles [12, 14, 15], where extensive information was provided on the local flow dynamics. These data have been reprocessed here such as extracting the bulk flow features required for evaluating the present model. The particles and the range of volume fractions investigated are the same as those studied in our recent work devoted to the sedimentation in a non-flowing condition [27]. The considered cases involved two samples of natural volcanic ash, Ash^1 and Ash^2, each made with particles of different shapes and sizes characterized by a specific size distribution, as well as a sample of almost spherical and monodisperse synthetic FCC

Experimental parameters	Ash^1	Ash^2	FCC
Solid particle density ρ_s (kg m^{-3})	1600	1490	1420
Mean particle equivalent diameter d (μm)	80	65	71
Particle volume fraction at packing Φ_{pack}	0.58	0.60	0.484
Range of particle volume fraction Φ_s	0.38−0.58	0.40−0.60	0.39−0.49

TABLE I. Properties of the materials used in the experiments.

particles (Table I). The materials were fully fluidized in the range of $0.65 \leq \Phi_s/\Phi_{pack} \leq 0.95$, then released down the channel until motion ceased (fig 2). In a first set of experiments ("*Set* 1"), performed with all different materials, Φ_s was varied from 0.6 to 0.38 by increasing the fluidization velocity, and so the height h_0 of the suspension, while the volume of particles was kept constant. In a second set of experiments ("*Set* 2"), performed with Ash^1, Φ_s was similarly ranged from 0.6 to 0.38 by varying the volume of particles whereas the initial height h_0 was fixed. Note also that the reservoir dimension (x_0=300 mm) and the channel width (w_0=150 mm) are much larger than the particle size (<250 μm), and that the settling of the particles lies in the Stokes regime.

III. PHYSICAL MODEL AND VALIDATION

In this section, we develop a physical description, from previous experimental observations described in section II, in the aim of formulating the model hypotheses that will allow us to derive mathematical relations between the main flow features and the final deposit. Then, we shall validate these predictions by comparison with experiments.

A. Hypotheses and predictions

Our flow model is based on the three following hypotheses.

- H1. The front velocity $U_{\mathcal{F}}$ remains constant during the whole flow duration.

- H2. During propagation, the suspension forms two distinct homogeneous and overlying layers, as illustrated in fig 1d: (1) at the bottom, a deposit of volume fraction Φ_{pack}

equal to both that of the initial random loosely packed bed (fig 1a) and that of the deposit obtained after defluidization in the non-flowing case (fig 1c); (2) above, a suspension, the volume fraction Φ_s of which remains constant during the flow and equal to that of the initial fluidized state (fig 1b).

- H3. Within the moving layer (fig 1d), the particles settle at a velocity U_{sed} that is the same as in a non flowing suspension (fig 1c).

Hypothesis H1 amounts to neglect the existence of the short acceleration and deceleration phases of the dam-break flow. The front velocity is thus equal to its average value, which is the ratio between the total length L traveled by the flow and its total duration T,

$$U_{\mathcal{F}} = \frac{L}{T}\,. \tag{2}$$

Hypotheses H2 and H3 imply together that the particle sedimentation velocity within the moving layer is given by eq 1 and only depends on the initial particle volume fraction Φ_s, the particles properties involved in U_{ref} and Φ_{pack}, and gravity acceleration. By considering the mass conservation of particles between a homogeneous suspension at concentration Φ_s and a deposit at concentration Φ_{pack}, these two hypotheses also lead to the following relation between the sedimentation velocity U_{sed} and the aggradation velocity U_{agg} of the deposit,

$$U_{agg} = \frac{U_{sed}}{\left(\frac{\Phi_{pack}}{\Phi_s} - 1\right)}\,. \tag{3}$$

Since the growth velocity of the deposit is constant, its height $h_d(x,t)$ can be obtained as the product of U_{agg} by the time t_d of deposition. In the reservoir ($x \leq x_0$), t_d is simply the time t elapsed since the stop of the gas supply. In the channel ($x > x_0$), it is the time taken between the gate opening and the considered distance reached by the mixture, $t_d = t - (x - x_0)/U_{\mathcal{F}}$. The deposit height is hence given by

$$h_d(x,t) = U_{agg}\, t \quad \text{for} \;\; x \leq x_0\,, \tag{4}$$

$$h_d(x,t) = U_{agg}\left(t - \frac{x - x_0}{U_{\mathcal{F}}}\right) \quad \text{for} \;\; x > x_0\,. \tag{5}$$

According to eqs 4-5, the shape of the deposit is represented by the dark gray zone on fig 1d-e. Within the reservoir, its top is a horizontal line located at a height that increases with time according to eq 4. Within the channel, it is a straight line with a negative slope

s that does not vary in time,

$$s = \frac{\partial h_d(x,t)}{\partial x} = -\frac{U_{agg}}{U_{\mathcal{F}}} = -\frac{T\,U_{sed}}{L}\left(\frac{1}{\frac{\Phi_{pack}}{\Phi_s}-1}\right). \tag{6}$$

At the end of the process (fig 1e), the shape of the final deposit is hence described by the juxtaposition of a rectangle of length x_0 and height $h_{d_\infty} = U_{agg}T$ with a triangle of height x_0 and length L. Since, according to hypothesis H2, their concentrations are the same, the mass conservation implies that the volume of final deposit is equal to that of the initial bed (fig 1a). This allows to relate the final deposit height, h_{d_∞}, to that of the initial packed bed, h_{d_0},

$$h_{d_\infty} = \beta h_{d_0} \quad \text{with} \quad \beta = \frac{x_0}{x_0 + \frac{L}{2}}\,, \tag{7}$$

Using eqs 4, 3 and 7, the total flow duration can be written as

$$T = \frac{h_{d_\infty}}{U_{agg}} = \frac{\beta\ h_{d_0}}{U_{agg}} = \frac{\beta\ h_{d_0}}{U_{sed}}\left(\frac{\Phi_{pack}}{\Phi_s}-1\right). \tag{8}$$

This result helps us to understand how the particle sedimentation and the dam-break flow combine to determine T. The dam-break flow stretches the gas-particle mixture by a factor $1/\beta > 1$ in the longitudinal direction and squeezes it by a factor $\beta < 1$ in the vertical direction. This deformation does not change the particle concentration that remains homogeneous, neither alters the particules settling that occurs at a constant velocity. However, the time it takes for the particles to settle is reduced by a factor β compared to the non-flowing case because the distance they travel to the bottom wall is reduced by the same amount. Since the flow lasts until all the particles have deposited, T is thus also reduced by a factor β.

B. Experimental validation

Now, we compare our model predictions with experimental results.

Figure 3 shows the experimental ratio $L/(TU_{\mathcal{F}_2})$ as a function of the normalized initial particle concentration Φ_s/Φ_{pack}. Whereas the front velocity significantly varies with the particle concentration, this ratio is remarkably constant and reasonably close to unity in all cases. We can therefore conclude that hypothesis H1 is reasonable. In the rest of this section, we consider a constant front velocity given by eq 2.

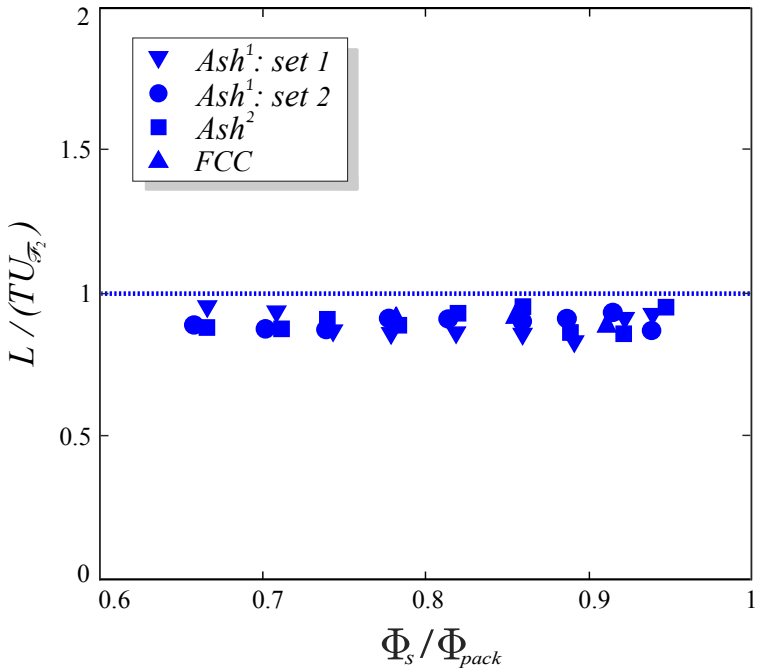

FIG. 3. Experimental ratio between the average front velocity , L/T, and the constant velocity of the second phase of the dam-break-flow, $U_{\mathcal{F}_2}$, as a function of Φ_s/Φ_{pack}, for all experiments.

Black curves in fig 4 show various experimental profiles of the final deposit in the channel ($x_0 \leq x \leq L$). In agreement with our model, the experimental deposits have almost a triangle shape. The blue curves are straight lines that connect the points of coordinates (0,βh_{d_0}) and (L,0), where the values of h_{d_0} and L are taken from the experiments. They fit the experimental profiles quite well, which confirms the validity of eq 7.

Figure 5 compares the experimental slopes of the final deposit, h_{d_∞}/L, to values calculated by means of eq 6, where U_{sed} is taken from non-flowing experiments at the same Φ_s/Φ_{pack}. Both these quantities, plotted on fig 5a as a fonction of Φ_s/Φ_{pack} for all experiments, strongly vary with the concentration. However, their ratio, plotted on fig 5b, is almost constant. It is slightly larger than unity because the average velocity L/T slightly underestimates the front velocity $U_{\mathcal{F}_2}$ of the second flow phase during which the velocity is truly constant (fig 3). This result confirms that eq 6 gives a good approximation of the relation between the deposit slope and the ratio between the front and sedimentation velocities.

Finally, we examine the total flow duration. Figure 6a shows the experimental values of T as a function of Φ_s/Φ_{pack}. We observe that T strongly depends on the particle concentration

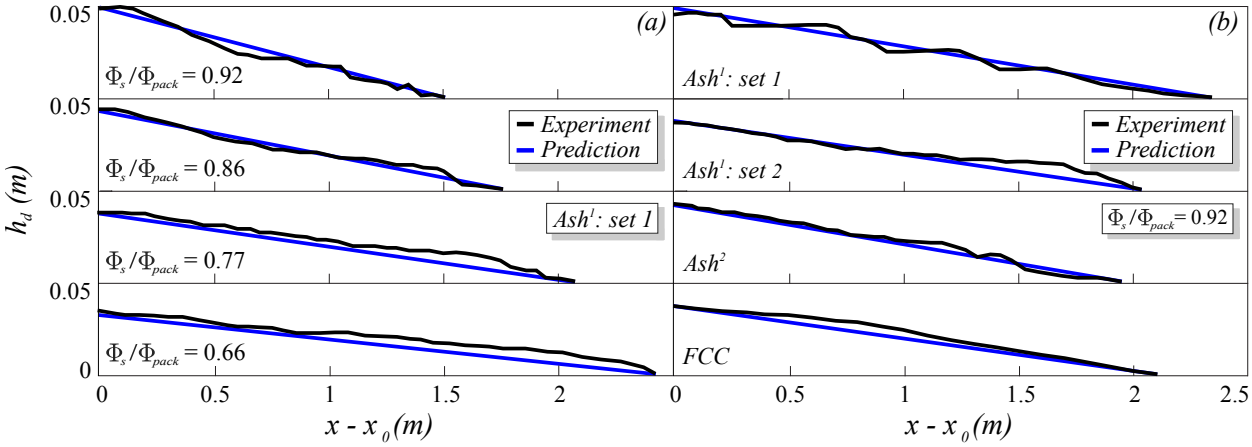

FIG. 4. Profiles of the final deposit within the channel ($x_0 \leq x \leq L$). Black curves, experimental data; blue lines, model prediction. (a) Ash^2 deposits obtained for different values of Φ_s/Φ_{pack}; (b) Ash^1, Ash^2, and FCC deposits obtained at a given value of $\Phi_s/\ \Phi_{pack}$.

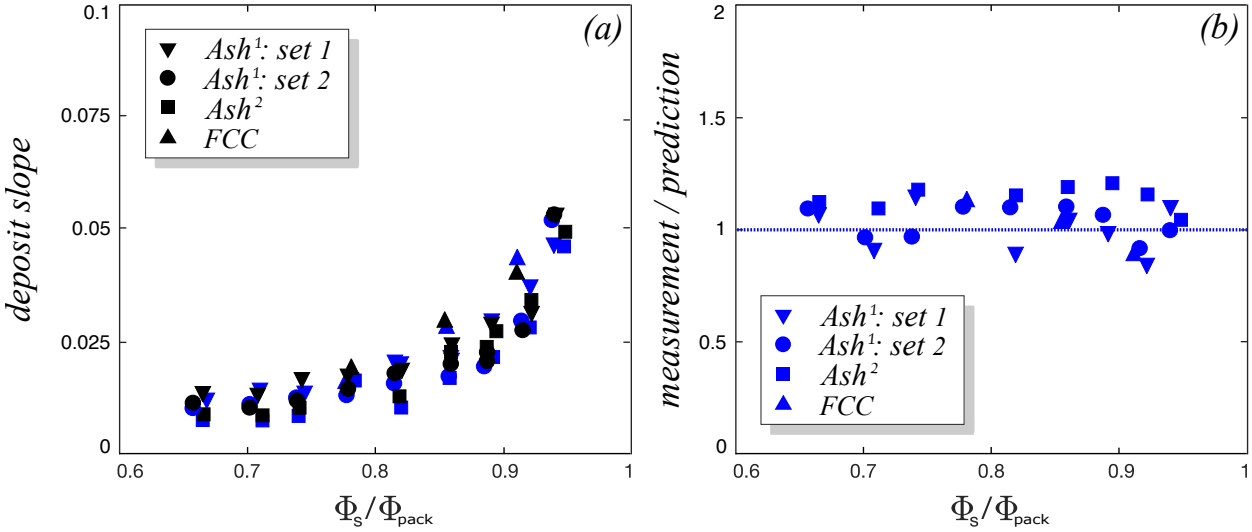

FIG. 5. Assessment of the model regarding the deposit slopes. (a) Measured deposit slopes $|h_{d_\infty}/L|$ (black symbols) and values predicted by eq 6 (blue symbols) as a function of Φ_s/Φ_{pack}, for all experimental cases. (b) Ratio between measured and predicted slopes.

and varies between the various cases involving different materials or test conditions. Figure 6b shows the ratio between the experimental values of T and those calculated by means of eq 8, where again the values of U_{sed} are taken from non-flowing experiments. This ratio remarkably gather the results around unity whatever the experimental conditions, confirming

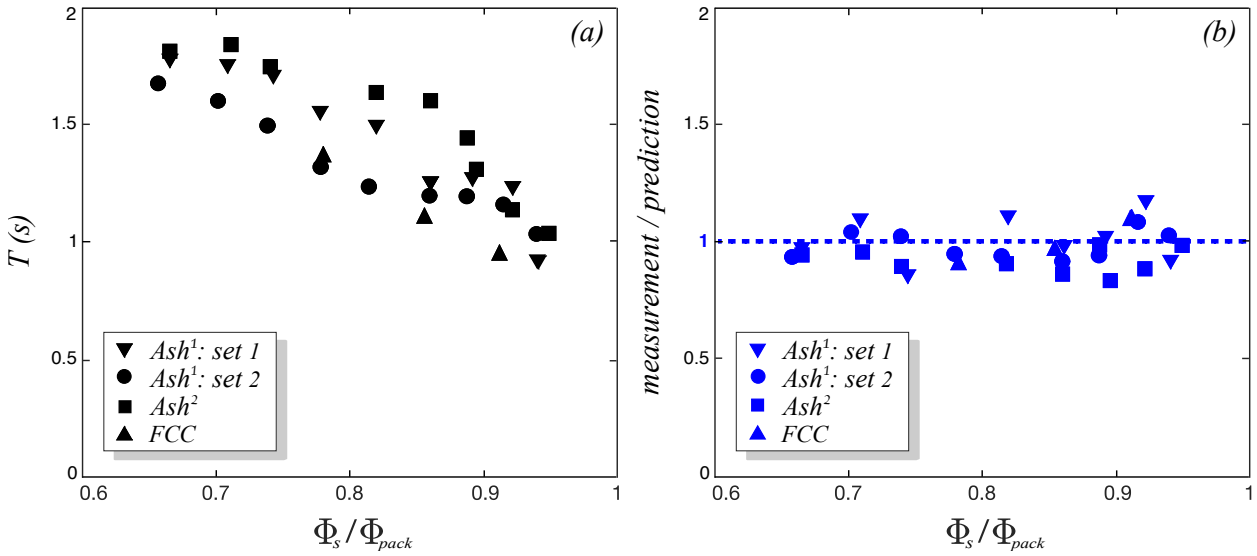

FIG. 6. Assessment of the model regarding the total duration T. (a) measured values of T as a function of Φ_s/Φ_{pack}, for all experiments. (b) Ratio between measured values of T and values predicted by eq 8.

the relevance of eq 8.

Despite the rather crude nature of hypotheses H1-3, the relations they allow to derive between the initial conditions before release, the global characteristics of the flow of the mixture and the geometry of the final deposit are in good agreement with experimental results. These hypotheses therefore draw a correct first approximation of the dam-break flow of sedimenting suspensions. The proposed relations thus constitute a reliable guide for the analysis of laboratory flows as well as natural ones.

IV. CONSEQUENCES ON THE MODELLING OF THE FLOW MIXTURE

We have analyzed the flow deposit left by a highly-expanded non-cohesive gas-particle suspension which has flowed in a horizontal straight channel. We showed that all the features of the final deposit, as well as the overall time duration of the flow, can be explained by assuming that the particle sedimentation is the same as that observed in a non-flowing homogeneous suspension which settles in a tank. That means that the sedimentation process is not influenced by the complex flow of the mixture through both the fluidization tank and the channel. It occurs at a constant velocity U_{sed} (hypothesis H3) while maintaining

a constant particle volume fraction (hypothesis H2). This conclusion has been obtained by taking advantage that the front velocity $U_{\mathcal{F}}$ of the dam-break flow in the investigated configuration remains constant during almost the entire process (hypothesis H1). However, in contrast with the sedimentation velocity which can be determined from the sole knowledge of the initial properties of the suspension [27], the dam-break flow does depend on the geometry of the channel. In particular, $U_{\mathcal{F}}$ is not expected to be constant in general and, for example, will change if the channel slope varies. The prediction of the profiles of the suspension height, $h(x,t)$, and of the average horizontal velocity of the mixture, $u(x,t)$, as well as the prediction of $U_{\mathcal{F}}(t)$ in any geometry, requires to solve the equations of mass and momentum conservation. Although the flow within the fluidization reservoir involves both significant horizontal and vertical velocities, the flow of the mixture within the channel is almost horizontal and can be described under the shallow-water approximation.

Shallow-water equations are commonly used to describe the flow of a heavy fluid into a lighter one [7], as well as that of a fluid laden by solid particles into the same fluid [31]. For a suspension of particles in a gas of negligible density flowing at high Reynolds number, the one-dimensional equations write:

$$\frac{\partial(\rho_m \delta_h)}{\partial t} + \frac{\partial(\rho_m \delta_h u)}{\partial x} = \dot{m}, \tag{9}$$

$$\frac{\partial(\rho_m \delta_h u)}{\partial t} + \frac{\partial(\rho_m \delta_h u^2)}{\partial x} + \frac{1}{2}\frac{\partial(\rho_m g \delta_h^2)}{\partial x} = \tau_p \ , \tag{10}$$

where u is the velocity of the mixture averaged over the thickness $\delta_h(x,t)$ of the moving layer, $\rho_m = \Phi_s \rho_s$ is the mixture density, $\dot{m}$ is the mass flux of particles that deposit and τ_p is the friction applied to the base of the flowing layer. In general, an additional equation is required to account for the evolution of the particle concentration [31]. However, for the type of flows under consideration, the concentration Φ_s remains constant throughout the flowing layer and equal to Φ_{pack} within the deposit. Note that shallow-water equations are more commonly formulated in terms of the whole height $h(x,t)$ of the gas-particle mixture, which is the sum of the height $h_d(x,t)$ of the growing deposit and the thickness $\delta_h(x,t)$ of the flowing mixture. Here, we have preferred to express them in terms of $\delta_h(x,t)$ because it is better suited to describe transfers between the deposit and the flowing layer. Moreover, the fact that the aggradation velocity is constant leads to a simple expression for the deposit

height,

$$\begin{cases} h_d(x,t) = 0 & \text{for } 0 \leq t \leq t_x, \\ h_d(x,t) = (t - t_x)U_{agg} & \text{for } t > t_x, \end{cases} \tag{11}$$

where t_x is the time taken for the front to reach the location x, which is equal to $(x - x_0)/U_{\mathcal{F}}$ in case the front velocity is constant. Once eqs 9-10 are solved, $h_d(x,t)$ and $h(x,t)$ can be easily determined by using eq 11.

The left-hand-sides of eqs 9-10 are known for a long time, but relevant expressions of $\dot{m}$ and τ_p are still lacking. Numerical simulations of the dam-break flow of a suspension in a channel based on shallow-water equations are presented in [25]. The solved equations are similar to eqs 9-10, but written in terms of $h(x,t)$ instead of $\delta_h(x,t)$. By modelling τ_p as a viscous friction, they could found a correct front velocity for phase 2 but largely overestimated the total time duration T of the flow. Finally, they introduced an additional solid friction to force the flow to stop in a reasonable time. Such a combination of solid and viscous frictions is often considered to interpret such flows [22, 32–34]. However, we have shown that T is not determined by the friction on the channel bottom but is controlled by the time taken by the particles to settle. The present results actually lead to simple expressions for $\dot{m}$ and τ_p when eqs 9-10 are written in terms of δ_h. The mass transfer from the moving layer to the deposited layer is given by the product of the aggradation velocity by the ratio between the volume fractions of these two layers,

$$\dot{m} = -\frac{\Phi_{pack}}{\Phi_s}\,\rho_m U_{agg} = -\frac{\Phi_{pack}}{(\Phi_{pack} - \Phi_s)}\,\rho_m U_{sed}\,. \tag{12}$$

The Reynolds number of the dam-break flow can be estimated by considering that the mixture can be described as an equivalent fluid of density ρ_m and viscosity μ_m. According to [27], the kinematic viscosity μ_m/ρ_m at large concentrations ($\Phi_s/\Phi_{pack} \approx 0.95$) hardly reaches that of water. The Reynolds number of the flow mixture is thus larger than 10^5 in laboratory experiments and much larger in natural flows. With such a large Reynolds number, the boundary layer is very thin. Considering that the mixture involves a plug flow above a fixed deposit is therefore a reasonable assumption, which is substantiated by the fact that the front velocity is observed to be constant in experiments performed in a horizontal channel. The momentum lost by the moving layer thus corresponds to the momentum lost by the particles that deposit, passing from a velocity u to rest, so that

$$\tau_p = \dot{m}\,u\,. \tag{13}$$

With this expressions of $\dot{m}$ and τ_p, and accounting for the fact that ρ_m is constant within the moving layer, eqs 9-10 can be simplified. By subtracting eq. 9 to eq. 10, it yields

$$\frac{\partial \delta_h}{\partial t} + \frac{\partial (\delta_h u)}{\partial x} = -\frac{\Phi_{pack}}{(\Phi_{pack} - \Phi_s)} U_{sed}, \tag{14}$$

$$\frac{\partial u}{\partial t} + u\frac{\partial u}{\partial x} + g\frac{\partial \delta_h}{\partial x} = 0. \tag{15}$$

Thus, when written in terms of δ_h, the equations describing the dam-break flow of a highly-expanded sedimenting suspension at large Reynolds number are similar to that of a pure inviscid fluid as expressed by [30], except for the right-hand-side of eq 14 which is responsible for the thinning of the moving layer due to continuous particle deposition. The reason why the right-hand-side of eq 15 is zero is that the shear stress τ_p reduces the momentum of the moving layer by decreasing its mass rather than its velocity.

Thus, combining eqs 14-15 with a model for the sedimentation velocity [27], should constitute the first-order approximation of a dense layer of pyroclastic flows along the major part of its course, excluding the initial formation which is fully three-dimensional and the very last stage, when the thickness of the boundary layer becomes comparable with that of the moving layer. Solving these equations is beyond the scope of this paper. However, it is interesting to estimate τ_p from experimental data by making some approximations about the flow in order to discuss the role it plays in the whole process.

The magnitude of τ_p can be evaluated by inserting the front velocity $U_{\mathcal{F}}$ in eq 13. Then normalizing by $\rho_s g d$, we can build a Shields number,

$$\mathrm{Sh} = \frac{\tau_p}{\rho_s g d}, \tag{16}$$

which compares the friction that forces a particle to stop when depositing with its weight. Figure 7a shows the experimental values of Sh. In all experimental configurations, Sh is mainly sensitive to the particle concentration, becoming four times larger when Φ_s/Φ_{pack} increases from 0.65 to 0.95. In any case, it is larger than 20, which means that the cohesion of the deposit is not due to gravity but necessarily results from the solid friction between the particles.

Another way to assess the role of τ_p is to analyze the respective contributions of the dam-break flow and of the sedimentation process to the total dissipation of mechanical energy. The total energy that is dissipated during each experimental test is equal to the

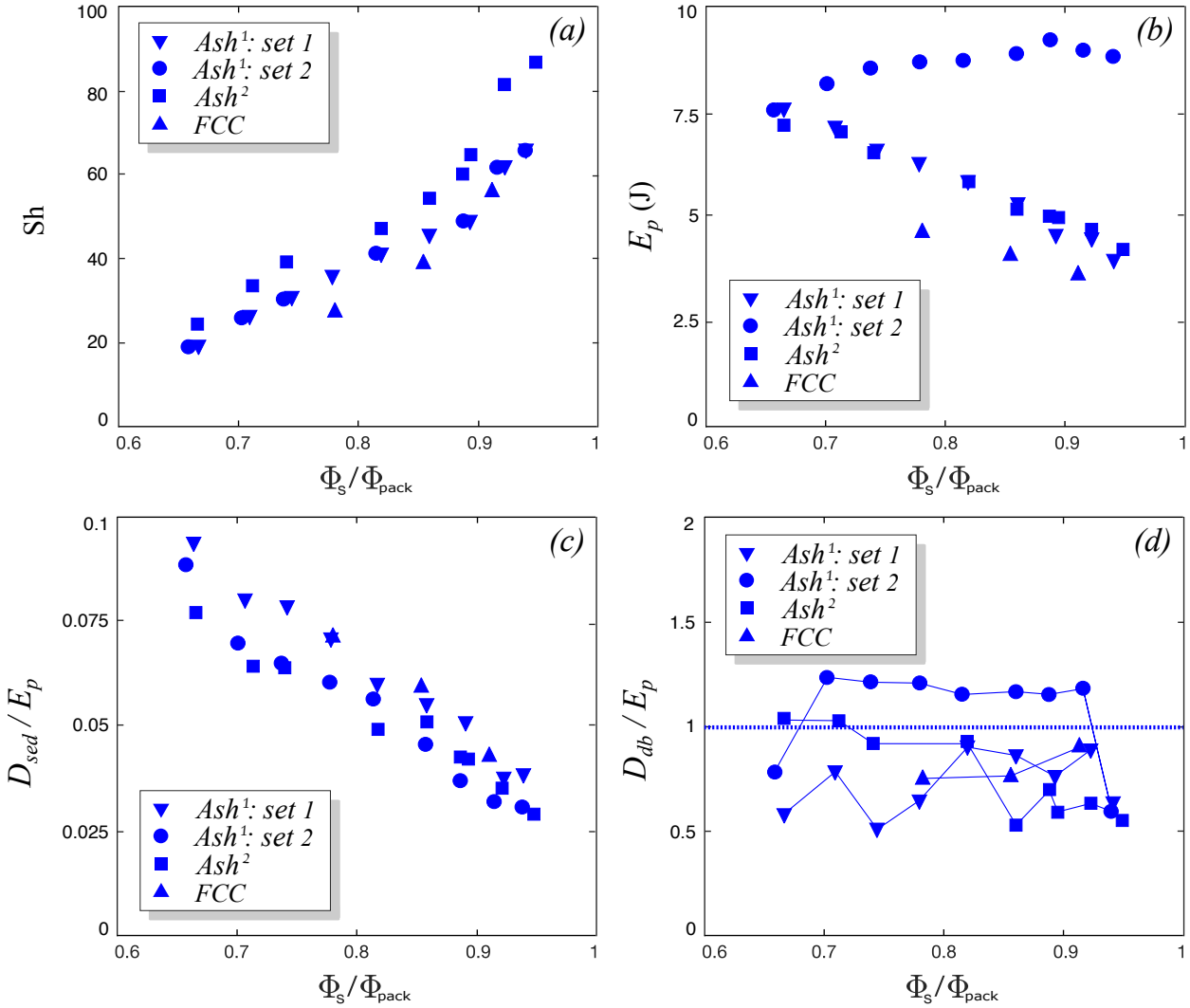

FIG. 7. Analysis of the wall friction τ_p and of its contribution to the dissipation from experimental data. (a) Shields number comparing wall friction to particle weight; (b) Potential energy E_p released during the total flow duration; (c) Energy D_{sed} dissipated by the sedimentation flow; (d) Energy D_{db} lost by dam-break flow due to τ_p, calculated under the assumption of a linear longitudinal velocity profile (eq. 21).

potential energy of gravity that is released between the beginning and the end of the flow: $E_p = Mg(h_{g0} - h_{gd})$, where M is the total mass of particles, h_{g0} the elevation of the center of mass of the fluidized mixture before its release in the channel (fig 1b), and h_{gd} that of the final deposit (fig 1e). The value of E_p, which can easily be calculated from experimental data, is plotted in fig 7b. Note that it varies significantly according to experimental conditions.

Then, we consider the sedimentation process. The dissipation rate per unit volume ε_{sed} during fluidization experiments within the initial reservoir – with the gate to the channel closed – can be obtained as the product of the fluidization velocity, U_g, by the pressure gradient within the bed of particles, $\Phi_s \rho_s g$. Since fluidization and sedimentation processes were shown to be equivalent for a homogeneous suspension [27], the dissipation during the sedimentation process is given by the same expression with taking U_{sed} in place of U_g,

$$\varepsilon_{sed} = \Phi_s \rho_s g U_{sed} \, . \tag{17}$$

Because the sedimentation is independent of the dam-break flow, the value of ε_{sed} given by eq 17 is still relevant for the flowing suspension. The energy dissipated by the sedimentation process is therefore

$$D_{sed} = \varepsilon_{sed} \int_0^T \vartheta(t) dt, \tag{18}$$

where the volume $\vartheta(t)$ of the suspension at instant t is its initial volume ϑ_0 minus the deposited volume,

$$\vartheta(t) = \vartheta_0 + \int_0^T \frac{\dot{m}}{\rho_m} \, w_0 \, x_{\mathcal{F}}(t) dt \, , \tag{19}$$

where $x_{\mathcal{F}}(t) = (x_0 + U_{\mathcal{F}} \, t)$ is the position of the front and w_0 the width of the channel. Values of D_{sed}, computed by applying eqs 17-19 to experimental data and normalized by E_p, are plotted in fig 7c. It is interesting to note that the results of the four cases are similar despite significant differences in the total dissipated energy. D_{sed} strongly decreases with Φ_s/Φ_{pack}, which indicates that it is mainly controlled by the particle concentration. However, in any case, the sedimentation contributes less than 10% of the total dissipation.

Now, let us consider the mechanical energy that is lost by the dam-break flow because of τ_p,

$$D_{db} = - \int_{x0}^{L} \int_{\frac{x-x_0}{U_{\mathcal{F}}}}^{T} w_0 \, \tau_p \, u(x,t) \, dt dx \, . \tag{20}$$

Since we do not know the velocity profile in the experiments, we propose to estimate D_{db} by assuming a linear evolution between the reservoir wall at $x = 0$ and the front position $x_{\mathcal{F}}(t)$ which moves at constant velocity $U_{\mathcal{F}}$,

$$u(x,t) = (x/x_{\mathcal{F}}(t)) \; U_{\mathcal{F}} \, . \tag{21}$$

It is a crude assumption, which is however probably a reasonable first-order approximation since the mixture surface $h(x)$ is observed to be rather smooth and regular (fig 2). Values of D_{db}, computed from experimental data by means of eqs 21-20, are plotted in fig 7d. Despite the assumption made regarding the velocity profile and the fact that our model is not expected to be valid during the first and the last stages of the flow, D_{db}/E_p is found to be of the order of unity. Moreover, it remains roughly constant with Φ_s/Φ_{pack} whereas E_p varies significantly. We can thus conclude that the present model of τ_p is consistent with the experimental data.

V. CONCLUDING REMARKS

The lower layer of pyroclastic flows is made of a gas laden with fine non-cohesive ash particles. Its properties can be investigated by means of laboratory experiments. By revisiting the characteristics of the final deposit and the total time duration measured in such experiments, distinctive properties of these flows have been revealed, which shed light on their dynamics and draw guidelines for the modelling of natural flows of ash generated by a volcanic eruption.

The most striking feature of such flows is the absence of a significant coupling between the sedimentation process and the overall flow of the mixture. Both the volume fraction and the sedimentation velocity of the particles are found not to be influenced by the rapid flow in the channel, which however involves a strong elongation of the mixture in the longitudinal direction. This means that the particle concentration, Φ_s, of the flowing mixture can be considered to be constant in space and time. Also, it implies that the sedimentation velocity, U_{sed}, is the same as that measured in a non flowing mixture confined within a reservoir, which has been modeled in a previous work as a function of the ratio Φ_s/Φ_{pack} between the particle volume fraction and its value at packing [27]. Because Φ_s is constant, the mass flux, $\dot{m}$, of particles that settle down and the growth velocity, U_{agg}, of the deposit are directly related to U_{sed} and can be determined from Φ_s/Φ_{pack}.

Furthermore, the mixture can be described as an equivalent fluid of constant density ρ_m and viscosity μ_m. The Reynolds number of the flow mixture is larger than 10^5 in laboratory experiments and much larger in natural flows. In addition, the contribution of the sedimentation process to the dissipation of mechanical energy turns out to be small. Therefore, the

mixture can be reasonably approximated as inviscid and moving as a plug flow at velocity u. The momentum flux that leaves the flowing mixture is thus determined by the momentum lost by the particles as they deposit, $\tau_p = \dot{m}u$.

During the longest part of their run, such flows are quasi-parallel and the evolution of both the thickness and the velocity of the moving mixture can be described by shallow-water equations including $\dot{m}$ and τ_p as sink terms of mass and momentum, respectively. The present analyzis of experiments performed in a horizontal channel indicates that this should lead to a good prediction of the total flow duration and of the deposit shape, provided that the front velocity is correct. In addition, numerical solving of shallow-water equations for an inviscid fluid in a similar geometry leads to a constant front velocity in agreement with experiments [25]. We are therefore confident that shallow water equations with the sink terms proposed here constitute a good tool to predict natural flows of hot dense volcanic ash in any geometry with smooth slope variations, as it is the case when such flows travel down valleys.

Beyond the fact that these equations allow to compute the complete longitudinal evolution of the horizontal velocity and that of the mixture height, the findings of this study can provide precious hints for the interpretation of the geologist's field measurements. As an illustration, let us consider that the following quantities can be estimated from the analysis of sediments: the total run-out distance L, the thickness of the deposit h_{d_∞}, and the slope of the deposit s. Then, if the properties of the ash particles (size, density, packing fraction Φ_{pack}) can be determined from the analysis of the sediments, the relation between the aggradation velocity, U_{agg}, and the particle volume fraction, Φ_s, of the flowing mixture can be estimated. Combining the results of this study, we have the four following relations, $U_{agg} = f(\Phi_s/\Phi_{pack})$, $s = U_{agg}/U_{\mathcal{F}}$, $h_{d_\infty} = TU_{agg}$ and $U_{\mathcal{F}} = L/T$, from which the four unknowns Φ_s, U_{agg}, $U_{\mathcal{F}}$ and T can be evaluated. Of course, if the flow dynamics is computed from shallow-water equations, variations of the topography of the valley can be taken into account to interpret variations of the flow deposit along the flow path.

---

[1] M. R. Rampino and S. Self, Volcanic winter and accelerated glaciation following the Toba super-eruption, Nature **359**, 50 (1992).

[2] A. Robock, Volcanic eruption and climate, Review Geophys. **38**, 191 (2000).

[3] S. Dartevelle, G. G. Ernst, J. Stix, and A. Bernard, Origin of the Mount Pinatubo climactic eruption cloud: Implications for volcanic hazards and atmospheric impacts, Geology **30**, 663 (2002).

[4] J. W. Rottman and J. E. Simpson, Gravity currents produced by instantaneous releases of a heavy fluid in a rectangular channel, J. Fluid Mech. **135**, 95 (1983).

[5] J. E. Simpson, *Gravity Currents in the Environment and the Laboratory*, 2^{nd} ed., Vol. 1 (Cambridge Univ. Press, New York, Cambridge, 1997).

[6] I. Eames and M. A. Gilbertson, Aerated granular flow over a horizontal rigid surface, J. Fluid Mech. **424**, 169 (2000).

[7] A. J. Hogg and D. Pritchard, The effects of hydraulic resistance on dam-break and other shallow inertial flows, J. Fluid Mech. **501**, 179 (2004).

[8] O. Roche, M. A. Gilbertson, J. C. Phillips, and R. S. J. Sparks, Experimental study of gas-fluidized granular flows with implications for pyroclastic flows emplacement, J. Geophys. Res. **109**, 201 (2004).

[9] É. Lajeunesse, J.-B. Monnier, and G. M. Homsy, Granular slumping on a horizontal surface, Phys. Fluids **17**, 1 (2005).

[10] A. J. Hogg, Lock-release gravity currents and dam-break flows, J. Fluid Mech. **569**, 61 (2006).

[11] M. Cantero, J. R. Lee, S. Balachandar, and G. Marcelo, Granular collapse in a fluid: Role of the initial volume fraction, J. Fluid Mech. **586**, 1 (2007).

[12] L. Girolami, T. H. Druitt, O. Roche, and Z. Khrabrykh, Propagation and hindered settling of laboratory ash flows, J. Geophys. Res. **113**, B02202 (2008).

[13] L. Girolami, *Dynamique et sédimentation des écoulements pyroclastiques reproduits en laboratoire*, Ph.D. thesis, Université de Clermont II (2008).

[14] L. Girolami, O. Roche, T. H. Druitt, and T. Corpetti, Particle velocity fields and depositional processes in laboratory ash flows, with implications for the sedimentation of dense pyroclastic flows, Bull Volcanol **72**, 747 (2010).

[15] L. Girolami, T. H. Druitt, and O. Roche, Towards a quantitative understanding of pyroclastic flows: Effects of expansion on the dynamics of laboratory fluidized granular flows, J. Volcanol. Geotherm. Res. **296**, 31 (2015).

[16] F. Dobran, A. Neri, and M. Todesco, Assessing the pyroclastic flow hazard at Vesuvius, Nature

367, 551 (1994).

[17] A. B. Clarke, B. Voight, A. Neri, and G. Macedonio, Transient dynamics of vulcanian explosions and column collapse, Nature **415**, 897 (2002).

[18] M. Todesco, A. Neri, T. E. Ongaro, P. Papale, G. Macedonio, R. Santacroce, and A. Longo, Pyroclastic flow hazard assessment at Vesuvius (Italy) by using numerical modeling. I. Large-scale dynamics, Bull. of Volcanology **64**, 155 (2002).

[19] A. Neri, T. Esposti-Ongaro, G. Macedonio, and D. Gidaspow, Multi-particle simulation of collapsing volcanic columns and pyroclastic flow, J. Geophys. Res. **108** (2003).

[20] S. Dartevelle, W. I. Rose, J. Stix, K. Kelfoun, and J. W. Vallance, Numerical modeling of geophysical granular flows: 2. Computer simulations of plinian clouds and pyroclastic flows and surges, Geoch., Geophys., Geosyst. **5** (2004).

[21] T. Esposti-Ongaro, S. Barsotti, A. Neri, and V.-S. Maria, *Large-eddy simulation of pyroclastic density currents*, Quality and Reliability of Large-Eddy Simulations, Vol. 161-170 (Springer, Dordrecht, 2011).

[22] E. E. Doyle, A. J. Hogg, H. M. Mader, and R. S. J. Sparks, Modeling dense pyroclastic basal flows from collapsing columns, Geophys. Res. Let. **35**, L04305 (2008).

[23] E. E. Doyle, A. J. Hogg, H. M. Mader, and R. S. J. Sparks, A two-layer model for the evolution and propagation of dense and dilute regions of pyroclastic currents, J. Volcanol. Geoth. Res. **190**, 365 (2010).

[24] C. Meruane, A. Tamburrino, and O. Roche, Dynamics of dense granular flows of small-and-large-grain mixtures in an ambient fluid, Phys. Rev. E, **86**, 02631 (2012).

[25] H. A. Shimizu, T. Koyaguchi, and Y. J. Suzuki, A numerical shallow-water model for gravity currents for a wide range of density differences, Progress in Earth and Planetary Science **4**, 209 (2017).

[26] D. Geldart, Types of gas fluidization, Powder Technology **7**, 285 (1973).

[27] L. Girolami and F. Risso, Sedimentation of gas-fluidized particles with random shape and size, Phys. Rev. Fluids **4**, 074301 (2019).

[28] L. Rondon, O. Pouliquen, and P. Aussillous, Granular collapse in a fluid: Role of the initial volume fraction, Phys Fluids **23**, 073301 (2011).

[29] O. Roche, S. Montserrat, Y. Nino, and A. Tamburrino, Experimental observations of water-like behavior of initially fluidized, dam break granular flows and their relevance for the propagation

of ash-rich pyroclastic flows, J. Geophys. Res. **113**, 4 (2008).

[30] M. Ungarish, A shallow-water model for high-Reynolds-number gravity currents for a wide range of density differences and fractional depths, Journal of Fluid Mechanics **579**, 373 (2007).

[31] R. T. Bonnecaze, H. E. Huppert, and J. R. Lister, Particle-driven gravity currents, Journal of Fluid Mechanics **250**, 339 (2006).

[32] E. E. Doyle, A. J. Hogg, and H. M. Mader, A two-layer approach to modelling the, Philos. Trans. R. Soc. Lond. A **467**, 1348 (2011).

[33] J. N. Procter, S. J. Cronin, T. Platz, A. Patra, K. Dalbey, M. Sheridan, and V. Neall, Mapping block-and-ash flow hazards based on Titan 2D simulations: a case study from Mt. Taranaki, NZ, Nat. Hazards **53**, 483 (2010).

[34] K. Kelfoun, Suitability of simple rheological laws for the numerical simulation of dense pyroclastic flows and long-runout volcanic avalanches, J. Geophys. Res.: Solid Earth **116**, B08209 (2011).